Title

Phenylalanine Mutation to Cyclohexylalanine Facilitates Triangular Trimer Formation by β-Hairpins Derived from Aβ.

Journal

Journal of the American Chemical Society, 142(49)

Authors

Haerianardakani, Sepehr
Kreutzer, Adam
Salveson, Patrick
et al.

Publication Date

2020-12-09

DOI

10.1021/jacs.0c09281

Peer reviewed

HHS Public Access

Author manuscript

J Am Chem Soc. Author manuscript; available in PMC 2021 December 09.

Published in final edited form as:

J Am Chem Soc. 2020 December 09; 142(49): 20708–20716. doi:10.1021/jacs.0c09281.

Phenylalanine Mutation to Cyclohexylalanine Facilitates Triangular Trimer Formation by β-Hairpins Derived from Aβ

Sepehr Haerianardakani[a], **Adam G. Kreutzer**[a], **Patrick J. Salveson**[a], **Tuan D. Samdin**[a], **Gretchen E. Guaglianone**[a], **James S. Nowick**[a,b]

[a]Department of Chemistry, University of California Irvine, Irvine, California 92697, United States

[b]Department of Pharmaceutical Sciences, University of California Irvine, Irvine, California 92697, United States

Abstract

Oligomers of the β-amyloid peptide, Aβ, play a central role in the pathogenesis and progression of Alzheimer's disease. Trimers and higher-order oligomers composed of trimers are thought to be the most neurotoxic Aβ oligomers. To gain insights into the structure and assembly of Aβ oligomers, our laboratory has previously designed and synthesized macrocyclic peptides derived from $A\beta_{17–23}$ and $A\beta_{30–36}$ that fold to form β-hairpins and assemble to form trimers. In the current study, we found that mutating Phe_{20} to cyclohexylalanine (Cha) in macrocyclic Aβ-derived peptides promotes crystallization of an Aβ-derived peptide containing the $A\beta_{24–29}$ loop (peptide $\mathbf{3_{F20Cha}}$) and permits elucidation of its structure and assembly by X-ray crystallography. X-ray crystallography shows that peptide $\mathbf{3_{F20Cha}}$ forms a hexamer. X-ray crystallography and SDS-PAGE further show that trimer $\mathbf{4_{F20Cha}}$, a covalently stabilized trimer derived from peptide $\mathbf{3_{F20Cha}}$, forms a dodecamer. Size exclusion chromatography shows that trimer $\mathbf{4_{F20Cha}}$ forms higher-order assemblies in solution. Trimer $\mathbf{4_{F20Cha}}$ exhibits cytotoxicity against the neuroblastoma cell-line SH-SY5Y. These studies demonstrate the use of the F20Cha mutation to further stabilize oligomers of Aβ-derived peptides that contain more of the native sequence and thus better mimic the oligomers formed by full-length Aβ.

Graphical Abstract

Corresponding Author: jsnowick@uci.edu.

Supporting Information

The Supporting Information is available free of charge on the ACS Publications website at https://pubs.acs.org.

Procedures for the synthesis of peptides **3**, $\mathbf{3_{F20Cha}}$, **4**, and $\mathbf{4_{F20Cha}}$ and trimers **2**, **2F20Cha**, and $\mathbf{4_{F20Cha}}$; screening and optimization of crystallization conditions and X-ray crystallographic data collection and structure determination; detailed descriptions of SDS-PAGE, CD, DLS, SEC, and LDH release assays.

The authors declare no competing financial interest.

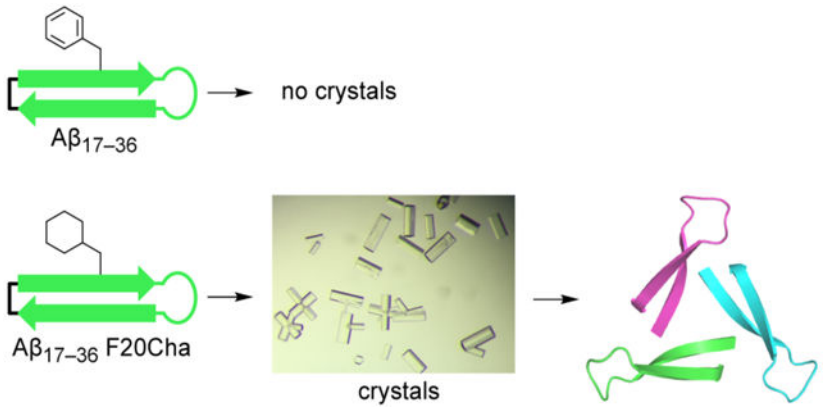

Introduction

Oligomers of the β-amyloid (Aβ) peptide are believed to be a key contributor to neurodegeneration in Alzheimer's disease.[1,2,3,4,5] Oligomers are soluble assemblies of Aβ that are in equilibrium with insoluble fibrils as well as monomers of Aβ. Although a unified model for the role of Aβ oligomers in Alzheimer's disease has not yet emerged, a variety of experiments have contributed to the current understanding of the structures and biology of Aβ oligomers.[6] Solid-state nuclear magnetic resonance (NMR) studies of Paravastu and coworkers showed that oligomers of Aβ are composed of antiparallel β-sheets.[7,8] Fourier transform infrared spectroscopic studies of Raussens and coworkers confirmed the formation of antiparallel β-sheets by $Aβ_{1–42}$.[9] Consistent with these structural models, NMR studies of Härd and coworkers have shown that $Aβ_{1–40}$ can adopt a β-hairpin conformation in solution when bound to an affibody.[10] Recently, NMR studies of Carulla and coworkers elucidated structure of a tetramer of $Aβ_{1–42}$ that further assembles to form an octamer.[11]

Electrophysiological studies of Selkoe and coworkers showed that trimers are the most potent inhibitors of long-term potentiation of neurons among low-n oligomers of Aβ.[12] Ashe and coworkers reported that Aβ dodecamers in brain extracts from the Alzheimer's disease mouse model Tg2576 initiate memory impairment.[13] Ion mobility mass spectrometric studies of Bowers and coworkers identified hexamers as a predominant assembly of $Aβ_{1–42}$.[14,15] Atomic force microscopy showed spherical hexamers, as well as dodecamers, as predominant assemblies formed by $Aβ_{1–42}$, which further assemble to form prefibrillar assemblies.[16] Native ion mobility mass spectrometric studies of Gräslund and coworkers showed that $Aβ_{1–42}$ forms hexamers in a membrane-like environment.[17] Further understanding the structures and assembly of oligomers promises to provide important insights into the molecular basis of Alzheimer's disease.

Our laboratory has pioneered the use of constrained peptide model systems to gain insights into the structures and assemblies of Aβ oligomers.[18] We previously designed and studied macrocyclic peptide **1**, which contains the heptapeptide sequences $Aβ_{17–23}$ and $Aβ_{30–36}$ and mimics an $Aβ_{17–36}$ β-hairpin.[19] Peptide **1** contains $Aβ_{17–23}$ and $Aβ_{30–36}$ β-strands linked by two δ-linked ornithine (^{δ}Orn) turn mimics (Figures 1A and B). The ^{δ}Orn connecting residues Asp_{23} and Ala_{30} replaces the $Aβ_{24–29}$ loop. The ^{δ}Orn connecting residues Leu_{17}

and Val_{36} reinforces β-hairpin structure. We incorporated an *N*-methyl group on the backbone of Phe_{20} to block uncontrolled aggregation of the peptide.[20] We replaced residue Met_{35} with the hydrophilic isostere ornithine (α-linked) to enhance the solubility of the peptide. X-ray crystallography revealed that three copies of peptide **1** assemble to form a triangular trimer, which further assembles to form hexamers and dodecamers.[19]

In a subsequent study, our laboratory covalently stabilized the triangular trimer formed by peptide **1** by mutating Leu_{17} and Ala_{21} to cysteine to create peptide **2**, which forms cross-linked trimer **2** upon oxidation with aqueous dimethyl sulfoxide (Figures 1A and D).[21] Although trimer **2** only contains *one third* of the natural Aβ peptide sequence, it shares biological properties with oligomers formed by full-length Aβ.

In studying derivatives of peptide **2**, we observed that mutating *N*-Me-Phe_{20} to *N*-Me-cyclohexylalanine (Cha) promotes crystallization, and thus facilitates elucidation of structure and assembly by X-ray crystallography. We also observed that the F20Cha mutation better facilitates the formation of cross-linked trimers derived from Aβ (Figure S1). The same effects did not occur when we mutated Phe_{19} of peptide **2** to Cha. Nilsson and coworkers have also observed that F20Cha mutation has marked effects the assembly of Aβ-derived peptides.[22] In studying $Aβ_{16–22}$, the researchers found that F20Cha mutation stabilizes fibril formation, while F19Cha mutation destabilizes fibril formation, suggesting the importance of interactions of Phe_{20} in stabilizing the assembly of Aβ.

In the current study, we set out to incorporate the missing $Aβ_{24–29}$ loop into peptide **1** and trimer **2** and exploit the F20Cha mutation to study the resulting peptides and trimers. We first incorporated the $Aβ_{24–29}$ loop into peptide **1** and found that the F20Cha mutation promotes crystallization and permits elucidation of the X-ray crystallographic structures of the peptide and oligomers that it forms (Figures 1B and C). We then used the F20Cha mutation to synthesize a cross-linked trimer that contains the $Aβ_{24–29}$ loop (Figure 1E), and we studied its X-ray crystallographic structure and assembly, as well as its biophysical and biological properties. These homologues, peptide $\mathbf{3_{F20Cha}}$ and trimer $\mathbf{4_{F20Cha}}$, contain more residues from Aβ than peptide **1** and trimer **2** and thus may better mimic full-length Aβ and the oligomers that it forms.

Results

The Effect of the F20Cha Mutation in Stabilizing β-Hairpin Peptides Containing the $Aβ_{24–29}$ Loop.

Our initial attempts to use X-ray crystallography to study the supramolecular assembly of Aβ-derived β-hairpin peptides containing the $Aβ_{24–29}$ loop failed. Peptide **3**, which is a homologue of peptide **1** containing the $Aβ_{24–29}$ loop, failed to grow crystals in any of the 576 crystallization conditions that we tested.[23] When we mutated Phe_{20} of peptide **3** to Cha, to create peptide $\mathbf{3_{F20Cha}}$, the peptide crystallized in at least seven different conditions that we tested, providing evidence that the F20Cha mutation helps promote crystallization of macrocyclic β-hairpin peptides derived from Aβ.

Crystallization, X-ray Crystallographic Structure, and Supramolecular Assembly of Peptide $\mathbf{3_{F20Cha}}$.

Peptide $\mathbf{3_{F20Cha}}$ afforded crystals suitable for X-ray diffraction in 0.1 M Bis-Tris buffer at pH 5.5, 0.1 M ammonium acetate, and 51% v/v 2-methyl-2,4-pentanediol. Diffraction data for peptide $\mathbf{3_{F20Cha}}$ were collected on a synchrotron at the Advanced Light Source. The X-ray crystallographic phases of peptide $\mathbf{3_{F20Cha}}$ were determined using single wavelength anomalous diffraction phasing (SAD phasing) from iodide atoms that were incorporated into the lattice by soaking crystals of the peptide in potassium iodide.[24] The X-ray crystallographic structure of peptide $\mathbf{3_{F20Cha}}$ reveals that the peptide assembles to form a triangular trimer, composed of three β-hairpins (Figures 2A and B).[25] The trimer has two hydrophobic surfaces — one surface contains side chains of the Phe_{19} residues and the other surface contains side chains of the Cha_{20} residues. We term these hydrophobic surfaces the "Phe_{19} face" and "Cha_{20} face" respectively. In the X-ray crystallographic structure of peptide $\mathbf{3_{F20Cha}}$, two triangular trimers further assemble to form a barrel-like hexamer (Figure 2C). In the barrel-like hexamer, the Cha_{20} faces of two trimers pack against each other, creating a hydrophobic core inside the hexamer. Hexamers formed by peptide $\mathbf{3_{F20Cha}}$ further pack on their Phe_{19} face to form columns in the crystal lattice.

The X-ray crystallographic studies of peptides **3** and $\mathbf{3_{F20Cha}}$ demonstrate that the F20Cha mutation enables stabilization of triangular trimers containing the $A\beta_{24–29}$ loop in the crystal state. The F20Cha mutation enhances the hydrophobicity of the Cha_{20} face, while maintaining similar steric interactions as the native Phe residue. We envision that the increased hydrophobicity of Cha_{20} face stabilizes trimers in the crystal state and thus highlights the importance of hydrophobic interactions in the formation of Aβ oligomers.

A Cross-Linked Trimer Containing the $A\beta_{24–29}$ Loop.

Our initial attempts to incorporate the $A\beta_{24–29}$ loop into trimer **2** were unsuccessful. In these initial attempts, we incorporated residues Val_{24}, Gly_{25}, Ser_{26}, Asn_{27}, Lys_{28}, and Gly_{29} of the $A\beta_{24–29}$ loop into the peptide **2** sequence, to create peptide **4** (Chart 1). Peptide **4** failed to form cross-linked trimer **4** upon oxidation with aqueous dimethyl sulfoxide (DMSO). HPLC analysis of the crude DMSO oxidation reaction mixture of peptide **4** shows a single peak corresponding to the monomer containing an intramolecular disulfide bond (Figure 3B). We hypothesized that mutating Phe_{20} to Cha in peptide **4**, to create peptide $\mathbf{4_{F20Cha}}$, would enable formation of cross-linked trimer $\mathbf{4_{F20Cha}}$, which contains the $A\beta_{24–29}$ loop. Peptide $\mathbf{4_{F20Cha}}$ forms cross-linked trimer $\mathbf{4_{F20Cha}}$ upon oxidation with aqueous DMSO. HPLC analysis of the crude oxidation reaction mixture of peptide $\mathbf{4_{F20Cha}}$ shows an additional HPLC peak corresponding to cross-linked trimer $\mathbf{4_{F20Cha}}$ in addition to a peak corresponding to the monomer containing an intramolecular disulfide bond (Figure 3A).

While optimizing the oxidation reaction of peptide $\mathbf{4_{F20Cha}}$, we observed that adding triethylamine (TEA) increases the yield of trimer $\mathbf{4_{F20Cha}}$. Preparative HPLC allows the isolation of pure trimer $\mathbf{4_{F20Cha}}$ from the reaction mixture. Thus, oxidation of 32 mg of peptide $\mathbf{4_{F20Cha}}$ afforded ca. 7 mg (22%) of pure trimer $4_{\mathbf{F20Cha}}$. The successful formation of trimer $\mathbf{4_{F20Cha}}$ corroborates that the $A\beta_{24–29}$ loop can be accomodated in the structure of cross-linked trimers derived from Aβ.

Crystallization, X-ray Crystallographic Structure, and Supramolecular Assembly of Trimer $\mathbf{4_{F20cha}}$.

To ascertain the effect of the $A\beta_{24–29}$ loop on the structure and supramolecular assembly of cross-linked trimers derived from Aβ, we turned to X-ray crystallography. Previous X-ray crystallographic studies showed that four copies of trimer **2** or trimer $\mathbf{2_{F20Cha}}$ further assemble to form ball-shaped dodecamers.[21, 26] Trimer $\mathbf{4_{F20Cha}}$ afforded crystals suitable for X-ray diffraction in conditions similar to those that we had previously used to crystallize trimers **2** and $\mathbf{2_{F20Cha}}$ — 0.1 M Tris buffer at pH 8.75, 0.2 M $MgC1_2$, and 2.6 M 1,6-hexanediol. X-ray diffraction data were collected on an X-ray diffractometer with a copper anode at 1.54 Å. The X-ray crystallographic structure of trimer $\mathbf{4_{F20Cha}}$ was determined by molecular replacement using trimer **2** as a search model.

The X-ray crystallographic structure of trimer $\mathbf{4_{F20Cha}}$ is similar to that of trimer **2** and trimer $\mathbf{2_{F20Cha}}$, with three folded β-hairpins linked in a triangular arrangement by disulfide bonds (Figure 4).[21, 26] Trimer $\mathbf{4_{F20Cha}}$ displays three loops and two hydrophobic surfaces (Figures 4A and B). Four copies of the trimer further assemble to form a ball-shaped dodecamer, with the Cha_{20} faces of the four trimers lining the interior of each dodecamer, creating a hydrophobic core (Figure 4C).

The X-ray crystallographic structure of trimer $\mathbf{4_{F20Cha}}$ corroborates that the F20cha mutation promotes the formation of a cross-linked trimer containing the $A\beta_{24–29}$ loop and that the trimer retains a triangular structure. Trimer $\mathbf{4_{F20Cha}}$ assembles to form a dodecamer that resembles the dodecamers formed by trimers **2** and $\mathbf{2_{F20Cha}}$. The propensity of trimer $\mathbf{4_{F20Cha}}$ to assemble to form a dodecamer demonstrates that incorporating the $A\beta_{24–29}$ loop into the cross-linked trimers derived from Aβ does not alter assembly, suggesting that the supramolecular assembly is governed by interactions of the β-sheet regions formed by $A\beta_{17–23}$ and $A\beta_{30–36}$. Trimer $\mathbf{4_{F20Cha}}$ contains more of the natural Aβ peptide sequence than trimer **2** and should thus better mimic trimers and higher-order oligomers that full-length Aβ may form.

Biophysical and Biological Studies of Peptides Containing the $A\beta_{24–29}$ Loop.

We turned to SDS-PAGE, circular dichroism (CD) spectroscopy, dynamic light scattering (DLS), and size exclusion chromatography (SEC) to determine whether the assemblies observed crystallographically form in solution. We also studied cytotoxicity, using the neuroblastoma cell-line SH-SY5Y, to investigate the effect of the $A\beta_{24–29}$ loop and the F20cha mutation on the cytotoxicity of the cross-linked trimers and the β-hairpin peptides.

SDS-PAGE.—In SDS-PAGE, the 6.6 kDa trimer $\mathbf{4_{F20Cha}}$ migrates as a band close to the 26 kDa size standard, which is consistent with the molecular weight of a 26.4 kDa dodecamer (Figure 5). The 5.1 kDa trimer **2** migrates as an elongated band between the 17 and 26 kDa size standards, suggesting a dodecamer in equilibrium with lower order oligomers such as hexamers and nonamers.[21] The band formed by trimer $\mathbf{4_{F20Cha}}$ also shows a diffuse feature below the 17 kDa sized standard, suggesting that the 26.4 kDa dodecamer may be in slow equilibrium with a hexamer or an equilibrating mixture of hexamers and nonamers. The band formed by trimer $\mathbf{2_{F20Cha}}$ shows a pronounced feature close to the 26 kDa size

standard, as well as downward streaking. The feature close to the 26 kDa size standard suggests the formation of a dodecamer (20.4 kDa) or pentadecamer (25.5 kDa), while the streaking suggests equilibria with lower order oligomers. The contrast in appearance of the bands formed by trimer $\mathbf{2_{F20Cha}}$ and trimer **2** further supports that the F20Cha mutation stabilizes higher-order oligomers.[26] In contrast to the trimers, peptides **3** and $\mathbf{3_{F20Cha}}$ migrate as single bands between the 1.7 kDa and 4.6 kDa size standards, which are consistent with molecular weights of monomers (2.2 kDa) or possibly dimers (4.4 kDa).

Circular Dichroism.—We initially performed CD experiments in phosphate buffer at pH 7.4. In phosphate buffer, the CD spectra of trimers **2**, $\mathbf{2_{F20Cha}}$, and $\mathbf{4_{F20Cha}}$ show minima near 210 nm (Figure 6A). In contrast, the CD spectra of peptides **1**, **3**, and $\mathbf{3_{F20Cha}}$ show sharp minima near 200 nm, with shallow negative ellipticity from ca. 210–240 nm (Figure 6B). Although none of the CD spectra match ideal β-sheet or random coil spectra, the CD spectra of trimers **2**, $\mathbf{2_{F20Cha}}$, and $\mathbf{4_{F20Cha}}$ more closely match a canonical β-sheet spectrum, while the CD spectra of peptides **1**, **3**, and $\mathbf{3_{F20Cha}}$ more closely match a canonical random coil spectrum.[27] These observations are consistent with our previous finding that covalent stabilization of triangular trimers promotes folding into β-hairpins.[21]

In performing CD experiments in phosphate buffer, we observed the formation of insoluble aggregates. To enhance the solubility of the peptides and trimers, we repeated the CD experiments in glycine buffer at pH 3.0. The minima for the CD spectra of trimers **2** and $\mathbf{2_{F20Cha}}$ do not substantially change between the neutral and acidic conditions (Figure 6C). Trimer $\mathbf{4_{F20Cha}}$ exhibits a substantially deeper minimum in glycine buffer than in phosphate buffer. This difference may reflect differences in the aggregation state of the peptide in the different buffer conditions.

Dynamic Light Scattering.—We turned to DLS to further investigate the aggregation state of the trimers. DLS provides an intensity-weighted analysis of aggregate size, with larger aggregates represented disproportionately with respect to monomers and small oligomers. We used phosphate buffer at pH 7.4 and glycine buffer at pH 3.0 to examine the effects of both neutral and acidic conditions. In phosphate buffer, DLS shows that trimer $\mathbf{4_{F20Cha}}$ forms assemblies with a hydrodynamic diameter of ca. 1000 nm (Figure 7A). In contrast, DLS shows that trimer $\mathbf{4_{F20Cha}}$ forms much smaller assemblies in glycine buffer, with a hydrodynamic diameter of ca. 10 nm (Figure 7B). Trimer **2** shows similar differences in phosphate and glycine buffers. In glycine buffer, DLS shows that trimer **2** forms assemblies with a hydrodynamic diameter of ca. 4 nm (Figure 7B), while in phosphate buffer, trimer **2** forms assemblies with a hydrodynamic diameter of ca. 500 nm (Figure 7A). These studies show that trimers $\mathbf{4_{F20Cha}}$ and **2** form large aggregates in phosphate buffer but much smaller assemblies or monomers in glycine buffer.

We repeated the DLS experiments, but with centrifuging of the peptide aliquots before acquiring the measurements. DLS shows that size of assemblies that trimers $\mathbf{4_{F20Cha}}$ and **2** form in phosphate buffer substantially decreases after centrifugation. Centrifugation removes the large aggregates and leaves only smaller assemblies in the solution. After centrifugation, the hydrodynamic diameters of the assemblies formed by trimers $\mathbf{4_{F20Cha}}$ and **2** in phosphate buffer decrease from ca. 1000 or 500 nm to ca. 10 or 100 nm, because

centrifugation removes most of the larger aggregates (Figure 7C). In contrast, centrifugation does not alter the size of the assemblies that trimers $\mathbf{4_{F20Cha}}$ and **2** form in glycine buffer (Figure 7D). We also measured the optical density (OD_{214}) of peptide aliquots before and after centrifugation. The optical density of peptide aliquots in phosphate buffer substantially decreases upon centrifugation, whereas the optical density of peptide aliquots in glycine buffer remains almost constant. This observation corroborates our finding that trimers $\mathbf{4_{F20Cha}}$ and **2** form large aggregates in phosphate buffer but smaller oligomers or monomers in glycine buffer.

Size Exclusion Chromatography.—We turned to size exclusion chromatography (SEC) to further probe the solution-phase assembly of the peptides and trimers. To ascertain the size of assemblies observed in SEC, we compared the elution profiles of the trimers and other peptides to the size standards blue dextran (2000 kDa), carbonic anhydrase (29 kDa), cytochrome C (12.4 kDa), aprotinin (6.5 kDa), and vitamin B12 (1.3 kDa). The size standards eluted from the column at 8.6, 11.7, 16.2, 18.8, and 19.3 mL, respectively (Figure S2).

Trimer $\mathbf{4_{F20Cha}}$ elutes as an elongated peak between 13.5 and 20.5 mL. In contrast, peptides **1**, **3**, and $\mathbf{3_{F20Cha}}$ and trimers **2**, and $\mathbf{2_{F20Cha}}$ elute after the vitaminB12 peak, with elution volumes from 19.5 to 22.0 mL (Figure 8). These large elution volumes are surprising, given that all the molecules exceed vitamin B12 in molecular weight. The anomalous elution volumes of peptides likely reflect adsorption to the polydextran SEC medium, which would retard their elution beyond that of small molecules. The elongated peak formed by trimer $\mathbf{4_{F20Cha}}$ is especially interesting and suggests that trimer $\mathbf{4_{F20Cha}}$ (6.6 kDa) is in equilibrium with higher-order assemblies, such as a hexamer (13.2kDa). In contrast, trimers **2** and $\mathbf{2_{F20Cha}}$ elute as single peaks at 21.2 and 20.8 mL respectively, suggesting that they do not assemble in glycine buffer at pH 3.0. The broadness and dramatically smaller elution volume of the peak formed by trimer $\mathbf{4_{F20Cha}}$ suggests that the $A\beta_{24–29}$ loop increases the propensity of trimer $\mathbf{4_{F20Cha}}$ to form higher-order assemblies. Peptides **3** and $\mathbf{3_{F20Cha}}$ elute as single peaks at 19.7 and 19.5 mL, respectively. The similar elution profiles of trimers **2** and $\mathbf{2_{F20Cha}}$, and of peptides **3** and $\mathbf{3_{F20Cha}}$, suggest that the F20Cha mutation does not alter the assemblies of Aβ-derived peptides under the conditions of SEC.[28,29]

LDH Release Assay.—To investigate whether the Aβ-derived peptides mimic the neurotoxicity of Aβ oligomers, we tested cytotoxicity of our peptides against the neuroblastoma cell-line SH-SY5Y using an LDH release assay. Trimers $\mathbf{4_{F20Cha}}$ and **2** induce cell death at 5–20 μM (Figure 9), while equivalent concentrations of peptides **3** and $\mathbf{3_{F20Cha}}$ do not (Figure S5). The toxicity of both trimers $\mathbf{4_{F20Cha}}$ and **2** decreases with trimer concentration. At equal concentrations, trimers $\mathbf{4_{F20Cha}}$ and **2** induce similar levels of cell death, suggesting that the $A\beta_{24–29}$ loop does not alter the toxicity of Aβ-derived peptides.[30]

Conclusions

Mutation of Phe_{20} to Cha facilitates the folding and assembly of macrocyclic peptides derived from Aβ. Replacement of *N*-Me-Phe in a β-hairpin peptide with *N*-Me-Cha ($\mathbf{3 \rightarrow 3_{F20Cha}}$) promotes crystallization as a triangular trimer that forms barrel-like hexamers.

This observation is consistent with our previous finding that the $A\beta_{24–29}$ loop can be accommodated in the structure of triangular trimers derived from Aβ.[31] The same mutation in a cysteine-containing homologue (**4**→**4**$_{\mathbf{F20Cha}}$) increases the efficiency of cross-linking to form triangular trimers. Although these studies do not directly reveal how Cha enhances the folding and assembly of these peptides, differences in properties between Phe and Cha must be responsible. Cha is substantially more hydrophobic than Phe and has been reported to enhance β-sheet formation.[32] Comparison of the CD spectra of peptide **1** and the Cha_{20}-containing homologue, peptide **1**$_{\mathbf{F20Cha}}$, confirms that mutating Phe to Cha increases the propensity of peptides to form β-sheets (Figure S6). It appears that the enhanced hydrophobicity and P-sheet forming propensity of Cha promote the formation of triangular trimers derived from Aβ.

Mutating Phe to Cha has enabled us to study Aβ-derived peptides and trimers containing the $A\beta_{24–29}$ loop. The incorporation of the $A\beta_{24–29}$ loop is significant, because these peptides and trimers contain almost one half of the natural Aβ peptide sequence. Aβ-derived peptides and trimers containing the $A\beta_{24–29}$ loop assemble in a similar fashion to those lacking it. Notably, trimers containing the $A\beta_{24–29}$ loop form a dodecamer in the crystal state and SDS-PAGE similar to their homologues lacking it, suggesting that the $A\beta_{24–29}$ loop neither prevents nor is necessary for the assembly of Aβ-derived peptides and trimers.

Peptide **3**$_{\mathbf{F20Cha}}$ and trimer **4**$_{\mathbf{F20Cha}}$ provide atomic-resolution X-ray crystallographic structures of trimers and dodecamers and mimic the propensity of Aβ to form trimers and the putative dodecamer Aβ*56.[13] We do not yet know if the trimers and dodecamers formed by peptide **3**$_{\mathbf{F20Cha}}$ and trimer **4**$_{\mathbf{F20Cha}}$ reflect the structures of biogenic Aβ oligomers. Indeed, these peptides contain many elements not present in Aβ — the δ-linked and α-linked ornithine, an *N*-methyl group, cyclohexylalanine, and in the case of trimer **4**$_{\mathbf{F20Cha}}$, disulfide crosslinks. Studies are now under way in our laboratory to address this important unanswered question.

Experimental Section

General Information

All chemicals were used as received except where noted otherwise. Methylene chloride (CH2CI2) was passed through alumina under argon in a solvent purification system prior to use. Anhydrous, amine free dimethylformamide (DMF) was purchased from Alfa Aesar. All reactions were performed at ambient temperature (ca. 20°C), unless otherwise noted. Analytical reverse-phase HPLC was performed on an Agilent 1200 equipped with an Aeris PEPTIDE 2.6 μm XB-C18 column (Phenomonex). Preparative reverse-phase HPLC was performed on a Rainin Dynamax equipped with a ZORBAX SB-C18 column (Agilent). HPLC grade acetonitrile and 18 MQ deionized water, each containing 0.1% trifluoroacetic acid (TFA), were used for analytical and preparative reverse-phase HPLC. Mass spectrometry was performed on a Waters Xevo G2-XS QTof mass spectrometer. All peptides were prepared and used as the trifluoroacetate salts and were assumed to have one trifluoroacetate ion per ammonium group present in each peptide.

Synthesis of peptides 1, 2, 2_{F20Cha}, 3, 3_{F20Cha}, 4, and 4_{F20Cha}

Peptides **1**, **2**, and $\mathbf{2_{F20Cha}}$ and were synthesized using protocols that our laboratory has previously described.[20,21,26] The syntheses of peptides **3**, $\mathbf{3_{F20Cha}}$, **4**, and $\mathbf{4_{F20Cha}}$ are modified from procedures that our laboratory has previously described and are described in detail in the Supporting Information.

Syntheses of cross-linked trimers 2, 2_{F20Cha}, and 4_{F20Cha}

Cross-linked trimers **2** and $\mathbf{2_{F20Cha}}$ were prepared by oxidizing peptides **2** and $\mathbf{2_{F20Cha}}$ using procedures that our laboratory has previously described.[21,26] Cross-linked trimer $\mathbf{4_{F20Cha}}$ was prepared by oxidizing peptide $\mathbf{4_{F20Cha}}$ (6 mM) in 20% aqueous DMSO in the presence of triethylamine (60 mM) as follows: the dry lyophilized peptide $\mathbf{4_{F20Cha}}$ was weighed and then transferred to a scintillation vial (20 mL) and dissolved in an appropriate volume of 20% (v/v) aqueous dimethyl sulfoxide (DMSO) to make a 6 mM solution of the peptide. An appropriate volume of triethylamine was added to the solution to make a 60 mM solution of triethylamine. The reaction mixture was incubated at ambient temperature (ca. 20°C) for two days. After incubation, the solution of the peptide was filtered through a 0.2 μm PVDF syringe filter, and the filtrate was injected into the RP-HPLC (20–50% ACN over 60 minutes) to purify cross-linked trimer $\mathbf{4_{F20Cha}}$. It is necessary to heat the HPLC column to 60°C during the purification of the cross-linked trimer.[33] In a typical procedure, oxidation of 32 mg of peptide $\mathbf{4_{F20Cha}}$ (as the TFA salt) afforded ca. 7 mg (22%) of trimer $\mathbf{4_{F20Cha}}$ (as the TFA salt) after HPLC purification and lyophilization.

Screening and optimization of crystallization conditions

Crystallization of peptides **3** and $\mathbf{3_{F20Cha}}$ and trimer $\mathbf{4_{F20Cha}}$ was attempted using protocols that our laboratory has previously published.[21,34] Stock solutions of peptides **3** and $\mathbf{3_{F20Cha}}$ and trimer $\mathbf{4_{F20Cha}}$ (10 mg/mL and 20 mg/mL) were prepared by dissolving 1.0 mg of dry lyophilized peptide in 100 μL or 50 μL of filtered 18 MΩ deionized water (NanoPure). The stock solutions were screened in 96-well plates using two kits from Hampton Research (Crystal Screen and Index). For each crystallization condition, three 150 nL hanging drops were prepared with well solution in 100:50, 75:75, and 50:100 ratio using a TTP LabTech Mosquito pipetting robot. For wells that gave promising crystals, the crystallization conditions were further optimized in a 4×6 matrix using a Hampton VDX 24-well plate by varying the pH and the concentration of cryoprotectant. For each of the crystallization conditions, three 2- or 3-μL hanging drops were prepared by mixing the peptide and crystallization solutions in 1:1, 1:2, and 2:1 ratios. Peptide **3** did not afford any crystals. In contrast, peptide $\mathbf{3_{F20Cha}}$ afforded crystals suitable for X-ray crystallography from a crystallization condition that was first identified on a 96-well plate and then optimized in 24-well plates. Trimer $\mathbf{4_{F20Cha}}$ did not grow crystals under the screening conditions, but afforded crystals suitable for X-ray crystallography in conditions similar to those we had previously published for trimer **2**.[21]

Data collection and structure determination

Initial diffraction data for peptide $\mathbf{3_{F20Cha}}$ were collected on a Rigaku Micromax-007HF X-ray diffractometer with a rotating copper anode at 1.54 Å wavelength with 0.5° oscillation.

Diffraction data were collected using CrystalClear. Diffraction data were scaled and merged using XDS. The X-ray crystallographic phases for peptide $\mathbf{3_{F20Cha}}$ were determined using single-wavelength anomalous diffraction (SAD) phasing by soaking a single crystal in a 1:1 mixture of 1 M potassium iodide and well solution.[24] Coordinates for the anomalous signal from the iodide ions were determined by HySS in the Phenix software suite 1.10.1. Electron density maps were generated using anomalous coordinates determined by HySS as initial positions in Autosol. Molecular manipulation of the model was performed with Coot. Coordinates were refined with phenix.refine.

Diffraction data for peptide $\mathbf{3_{F20Cha}}$ were also collected at the Advanced Light Source at Lawrence Berkeley National Laboratory with a synchrotron source at 1.00 Å wavelength to achieve higher resolution. The synchrotron diffraction data were scaled and merged using XDS. The electron density map was generated by molecular replacement using the coordinates from the structure of peptide $\mathbf{3_{F20Cha}}$ generated by soaking in KI using Phaser in the Phenix software suite 1.10.1. Molecular manipulation of the model was performed with Coot. Coordinates were refined with phenix.refine.

Data collection and structure determination of trimer 4_{F20Cha}

Diffraction data for trimer $\mathbf{4_{F20Cha}}$ were collected on a Rigaku Micromax-007HF X-ray diffractometer with a rotating copper anode at 1.54 Å wavelength with 0.5° oscillation. Diffraction data were collected using CrystalClear. Diffraction data were scaled and merged using XDS. The X-ray crystallographic phases for trimer $\mathbf{4_{F20Cha}}$ were determined by molecular replacement using trimer **2** as a search model in Phaser. Molecular manipulation of the model was performed with Coot. Coordinates were refined with phenix.refine.

SDS-PAGE

SDS-PAGE was performed in similar fashion to the protocols that our laboratory previously described.[26]

Circular dichroism spectroscopy

CD spectra were acquired on a JASCO-810 circular dichroism spectropolarimeter at ambient temperature (ca. 20°C). The spectra were acquired in similar fashion to the protocols that our laboratory previously described.[34]

Dynamic light Scattering

Dynamic light scattering was measured using a Malvern Zetasizer ZS Nano DLS at ambient temperature (ca. 20°C). Solutions of trimers (25 μM) were prepared in a similar fashion to the circular dichroism experiments and transferred to 1 cm disposable plastic cuvettes. Data were collected in 10 seconds time intervals and averaged over 3 measurements. The scattering was measured with a 173° backscattering angle. Dynamic light scattering was also measured after centrifugation of the solutions. In these experiments, the solutions were centrifuged at 14000 rpm (17000 × G) for 2 minutes, and then the supernatant was transferred to a plastic cuvette for DLS measurement. The optical density (OD_{214}) of each sample was measured before and after centrifugation using a Thermo Scientific NanoDrop

One microvolume UV-Vis spectrophotometer to monitor the loss of aggregates formed in buffered solutions of the cross-linked trimers (Table S2).

Size-exclusion Chromatography

All the SEC experiments were performed in 10 mM glycine containing 50 mM NaCl at pH 3.0 (adjusted with aq. HC1) at ambient temperature (ca. 20°C) on a GE Superdex 75 10/300 GL column. A 1.0 mg/mL solution of each cross-linked trimer was prepared by diluting 80 μL of 10 mg/mL stock solutions of each trimer in 720 μL of the glycine buffer in an Eppendorf tube (1.5 mL). We found that 1.0 mg/mL solutions of peptides **1**, **3**, and $\mathbf{3_{F20Cha}}$ were too concentrated and resulted in saturation of the detector (> 2.5 AU), thus 0.25 mg/mL solutions of peptides **1**, **3**, and $\mathbf{3_{F20Cha}}$ were used for SEC experiments. The solutions were centrifuged at 14000 rpm (17000 × G) for 2 minutes. After centrifugation, the supernatant of each peptide aliquot was injected to the column and run using a flow rate of 0.5 mL/min. Chromatograms were recorded at 214 nm and normalized to the maximum absorbance of the run. Size standards blue dextran, carbonic anhydrase, cytochrome C, aprotinin, and vitamin B12 were run in a similar fashion. The optical density (OD_{214}) of each sample was measured before and after centrifugation using a Thermo Scientific NanoDrop One microvolume UV-Vis spectrophotometer to monitor the loss of aggregates formed in buffered solutions of the peptides and cross-linked trimers (Table S3).

LDH release assay

LDH release assays were performed on the SH-SY5Y neuroblastoma cell-line, and cell death was quantified using procedures that our laboratory previously described.[21]

Supplementary Material

Refer to Web version on PubMed Central for supplementary material.

Acknowledgments

We thank the Laser Spectroscopy Labs at the University of California, Irvine for assistance with circular dichroism and dynamic light scattering measurements, the National Institutes of Health (NIH), National Institute of General Medical Sciences (NIGMS) for funding (Grant GM097562), and the Berkeley Center for Structural Biology (BCSB) of the Advanced Light Source (ALS) for synchrotron data collection. The BCSB is supported in part by the NIH, NIGMS, and the Howard Hughes Medical Institute. The ALS is supported by the Director, Office of Science, Office of Basic Energy Sciences, of the U.S. Department of Energy under Contract No. DE-AC02-05CH11231.

References

(1). Cleary JP; Walsh DM; Hofmeister JJ; Shankar GM; Kuskowski MA; Selkoe DJ; Ashe KH Natural oligomers of the amyloid-β protein specifically disrupt cognitive function. Nat. Neurosci 2005, 8, 79–84. [PubMed: 15608634]

(2). Walsh DM; Klyubin I; Fadeeva JV; Cullen WK; Anwyl R; Wolfe MS; Rowan MJ; Selkoe DJ Naturally secreted oligomers of amyloid β protein potently inhibit hippocampal long-term potentiation in vivo. Nature 2002, 416, 535–539. [PubMed: 11932745]

(3). Westerman MA; Cooper-Blacketer D; Mariash A; Kotilinek L; Kawarabayushi T; Younkin LH; Carlson GA; Younkin SG; Ashe KH The relationship between Aβ and memory in the Tg2576 mouse model of Alzheimer's disease. J. Neurosci 2002, 22, 1858–1867. [PubMed: 11880515]

(4). Selkoe DJ Alzheimer's disease is a synaptic failure. Science 2002, 298, 789–791. [PubMed: 12399581]

(5). Chimon S; Shaibat MA; Jones CR; Calero DC; Aizezi B; Ishii Y Evidence of fibril-like β-sheet structures in a neurotoxic amyloid intermediate of Alzheimer's β-amyloid. Nat. Struct. Mol. Biol 2007, 14, 1157–1164. [PubMed: 18059284]

(6). Cline EM; Bicca MA; Viola KL; Klein WL The amyloid-β oligomer hypothesis: beginning of the third decade. J. Alzheimer's Dis 2018, 64, 567–610.

(7). Tay WM; Huang D; Rosenberry TL; Paravastu AK The Alzheimer's amyloid-β (l-42) peptide forms off-pathway oligomers and fibrils that are distinguished structurally by intermolecular organization. J. Mol. Biol 2013, 425, 2494–2508. [PubMed: 23583777]

(8). Huang D; Zimmerman MI; Martin PK; Nix AJ; Rosenberry TL; Paravastu AK Antiparallel β-sheet structure within the C-terminal region of 42-residue Alzheimer's amyloid-β peptides when they form 150-kDa oligomers. J. Mol. Biol 2015, 427, 2319–2328. [PubMed: 25889972]

(9). Cerf E; Sarroukh R; Tamamizu-Kato S; Breydo L; Derclaye S; Dufrêne. Y. F.; Narayanaswami, V.; Goormaghtigh, E.; Ruysschaert, J. M.; Raussens, V. Antiparallel β-sheet: a signature structure of the oligomeric amyloid β-peptide. Biochem. J 2009, 421, 415–423. [PubMed: 19435461]

(10). Hoyer W; Grönwall C; Jonsson A; Ståhl S; Härd T Stabilization of a β-hairpin in monomeric Alzheimer's amyloid-β peptide inhibits amyloid formation. Proc. Natl. Acad. Sci. U.S.A 2008, 105, 5099–6104. [PubMed: 18375754]

(11). Ciudad S; Puig E; Botzanowski T; Meigoono M; Arango AS; Do J; Mayzel M; Bayoumi M; Chaignepain S; Maglia G; Cianferani S; Orekhov V; Tajkhorshid E; Bardiaux B; Carulla N Aβ(l-42) tetramer and octamer structures reveal edge conductivity pores as a mechanism for membrane damage. Nat. Commun 2020, 11, 3014. [PubMed: 32541820]

(12). Townsend M; Shankar GM; Metha T; Walsh DM; Selkoe DJ Effect of secreted oligomers of amyloid β-protein on hippocampal synaptic plasticity: a potent role for trimers. J. Physiol 2006, 572, 477–492. [PubMed: 16469784]

(13). Lesné S; Koh MT; Kotilinek L; Kayed R,; Glabe CG; Yang A; Gallagher M; Ashe KH A specific amyloid-β protein assembly in the brain impairs memory. Nature 2006, 440, 352–357. [PubMed: 16541076]

(14). Bernstein SL; Wyttenbach T; Baumketner A; Shea JE; Bitan G; Teplow DB; Bowers MT Amyloid β-protein: monomer structure and early aggregation states of $A\beta_{42}$ and its Pro^{19} alloform. J. Am. Chem. Soc 2005, 127, 2075–2084. [PubMed: 15713083]

(15). Bernstein SL; Dupuis NF; Lazo ND; Wyttenbach T; Condron MM; Bitan G; Teplow DB; Shea JE; Ruotolo BT; Robinson CV; Bowers MT Amyloid-β protein oligomerization and the importance of tetramers and dodecamers in the aetiology of Alzheimer's disease. Nat. Chem 2009, 1, 326–331. [PubMed: 20703363]

(16). Economou NJ; Giammona MJ; Do TD; Zheng X; Teplow DB; Buratto SK; Bowers MT Amyloid β-protein assembly and Alzheimer's disease: dodecamers of $A\beta_{42}$, but not of $A\beta_{40}$, seed fibril formation. J. Am. Chem. Soc 2016, 138, 1772–1775. [PubMed: 26839237]

(17). Österlund N; Moons R; Hag LL; Sobott F; Gräslund A Native ion mobility-mass spectrometry reveals the formation of β-barrel shaped amyloid-β hexamers in a membrance-mimicking environment. J. Am. Chem. Soc 2019, 141, 10440–10450. [PubMed: 31141355]

(18). Kreutzer AG; Nowick JS Elucidating the structures of amyloid oligomers with macrocyclic β-hairpin peptides: insights into Alzheimer's disease and other amyloid diseases. Acc. Chem. Res 2018, 51, 706–718. [PubMed: 29508987]

(19). Spencer RK; Li H; Nowick JS X-ray crystallographic structures of trimers and higher-order oligomeric assemblies of a peptide derived from $A\beta_{17–36}$. J. Am. Chem. Soc 2014, 136, 5595–5598. [PubMed: 24669800]

(20). Spencer R; Chen KH; Manuel G; Nowick JS Recipe for β-sheets: foldamers containing amyloidogenic peptide sequences. Eur J. Org. Chem 2013, 3523–3528.

(21). Kreutzer AG;Yoo S; Spencer RK; Nowick JS Stabilization, assembly, and toxicity of trimers derived from Aβ. J. Am. Chem. Soc 2017, 139, 966–975. [PubMed: 28001392]

(22). Senguen FT; Lee NR; Gu X; Ryan DM; Doran TM; Anderson EA; Nilsson BL Probing aromatic, hydrophobic, and steric effects on the self-assembly of an amyloid-β fragment peptide. Mol. BioSyst 2011, 7, 486–496. [PubMed: 21060949]

(23). Spencer RK; Nowick JS A newcomer's guide to peptide crystallography. Isr. J. Chem 2015, 55, 698–710. [PubMed: 26213415]

(24). Dauter Z; Dauter M; Rajashankar KR Novel approach to phasing proteins: derivatization by short cryo-soaking with halides. Acta Crystallogr., Sect.D: Biol.Crystallogr 2000, 56, 232–237. [PubMed: 10666615]

(25). β-Hairpins have also been observed in other oligomers from Aβ. For examples, see:(A)Yu L; Edalji R; Harlan JE; Holzman TF; Lopez AP; Labkovsky B; Hillen H; Barghorn S; Ebert U; Richardson. PL; Miesbauer L; Solomon L; Bartley D; Walter K; Johnson RW; Hajduk PJ; Olejniczak ET Structural characterization of a soluble amyloid beta-peptide oligomer. Biochemistry 2009, 48,1870–1877. [PubMed: 19216516] (B)Streltsov VA; Varghese JN; Masters CL; Nuttall SD Crystal structure of the amyloid-β p3 fragment provides a model for oligomer formation in Alzheimer's disease. J. Neurosci 2011, 31, 1419–1426. [PubMed: 21273426] (C)Ciudad S; Puig E; Botzanowski T; Meigooni M; Arango AS; Do J; Mayzel M; Bayoumi M; Chaignepain S; Maglia G; Cianferani S; Orekhov V; Tajkhorshid E; Bardiaux B; Carulla N Aβ(1-42) tetramer and octamer structures reveal edge conductivity pores as a mechanism for membrane damage. Nature Commun. 2020, 11, 3014. [PubMed: 32541820]

(26). Salveson PJ; Haerianardakani S; Thuy-Boun A;Yoo S; Kreutzer AG; Demeler B; Nowick JS Repurposing triphenylmethane dyes to bind to trimers derived from Aβ. J. Am. Chem. Soc 2018, 140, 11745–11754. [PubMed: 30125493]

(27). Trimer $\mathbf{4_{F20Cha}}$ exhibits a minima at a lower wavelength in glycine buffer than phosphate buffer. The lower wavelength of the minimum may suggest a lower degree of supramolecular assembly.

(28). A 0.25 mg/mL solution of trimer $\mathbf{4_{F20Cha}}$ elutes as a single peak at ca. 19.5 mL elution volume (Figure S3).$\mathbf{4_{F20Cha}}$

(29). We also attempted SEC experiments in Tris buffer at pH 7.4 to see the effect of neutral pH on the solution-phase assembly of the peptides and trimers. Trimer $\mathbf{4_{F20Cha}}$ forms high molecular weight aggregates that elute just after blue dextran under these conditions, indicating the formation oflarge assemblies (Figure S4).$\mathbf{4_{F20Cha}}$

(30). Trimer $\mathbf{4_{F20Cha}}$ and trimer **2** exhibit cytotoxicity at concentrations typical of Aβ oligomers. For a discussion of biologically relevant Aβ concentrations and the cytotoxicity of Aβ oligomers, see: Raskatov, J. A. ChemBioChem 2019, 20, 1725–1726. [PubMed: 30835961]

(31). Kreutzer AG; Spencer RK; McKnelly KJ; Yoo S; Hamza IL; Salveson PJ; Nowick JS A hexamer of a peptide derived from $A\beta_{16-36}$. Biochemistry 2017, 56, 6061–6071. [PubMed: 29028351]

(32). Tatko CD; Waters LM Selective aromatic interactions in β-hairpin peptides. J. Am. Chem. Soc 2002, 124, 9372–9373. [PubMed: 12167022]

(33). Yoo S; Zhang S; Kreutzer AG; Nowick JS An efficient method for the expression and purification of Aβ(M1-42). Biochemistry 2018, 57, 3861–3866. [PubMed: 29757632]

(34). Salveson PJ; Haerianardakani S; Thuy-Boun A; Kreutzer AG; Nowick JS Controlling the oligomerization state of Aβ-derived peptides with light. J. Am. Chem. Soc 2018, 140, 5842–5852. [PubMed: 29627987]

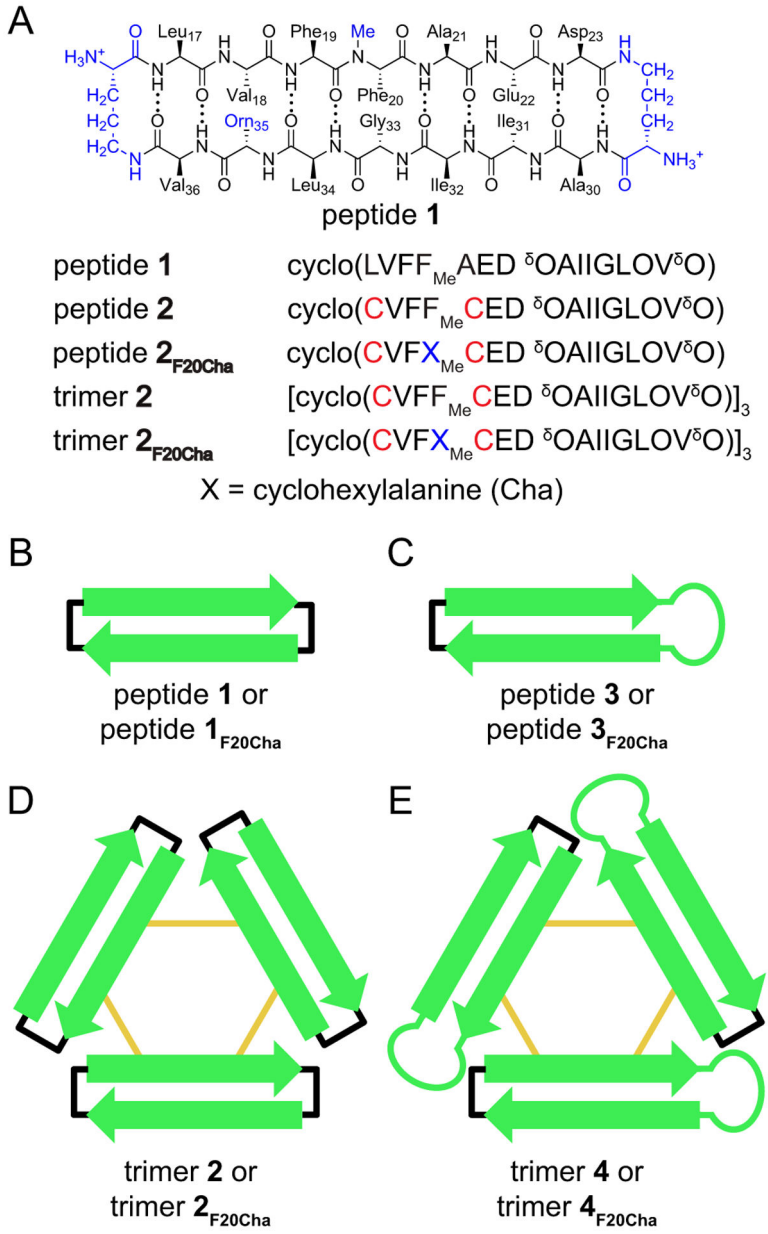

Figure 1.

Macrocyclic β-hairpin peptides and trimers derived from $A\beta_{17–36}$. (A) Chemical structure and amino acid sequences of peptide **1** and its homologues. (B) Cartoon structure of β-sheet peptides lacking the $A\beta_{24–29}$ loop. (C) Cartoon structure of β-hairpin peptides containing the $A\beta_{24–29}$ loop. (D) Cartoon structure of cross-linked trimers lacking the $A\beta_{24–29}$ loop. (E) Cartoon structure of cross-linked trimers containing the $A\beta_{24–29}$ loop. Yellow lines represent disulfide linkages, and black lines represent the $^{\delta}$Orn turn mimics.

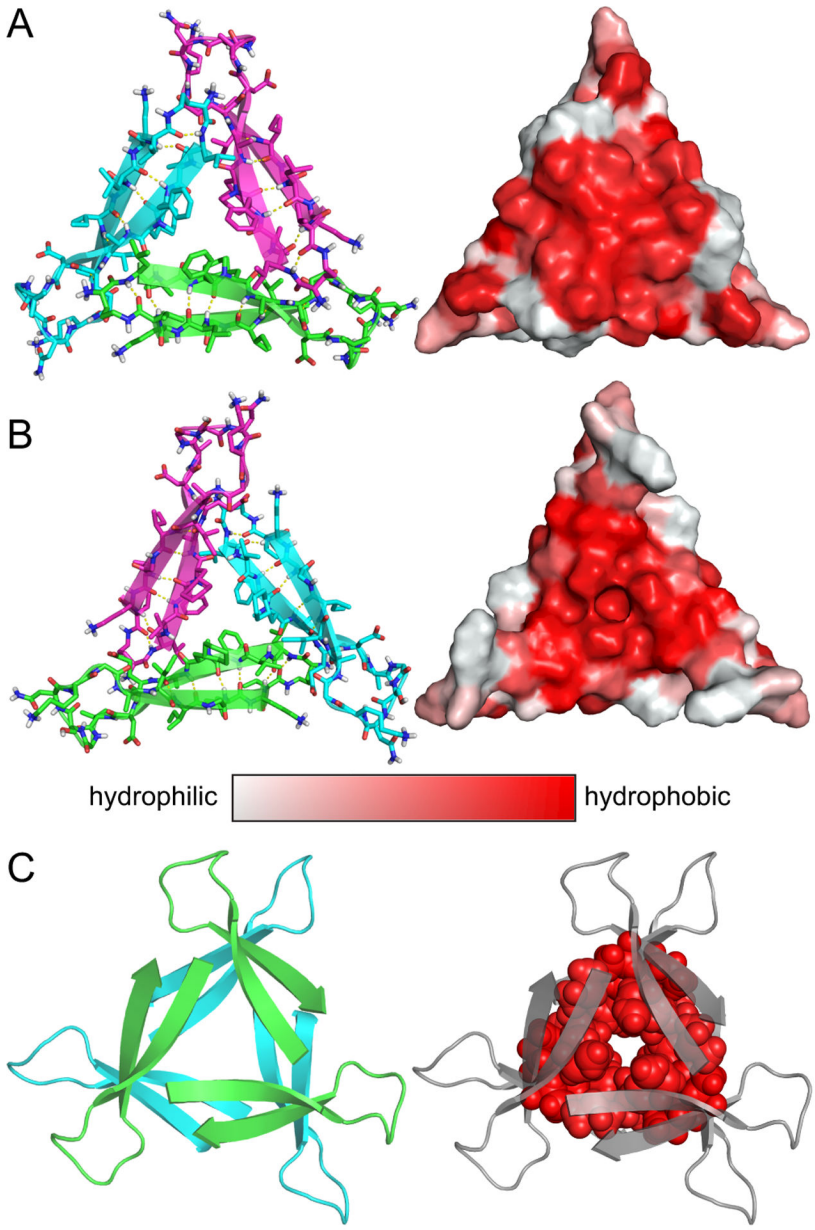

Figure 2.

The X-ray crystallographic structure of peptide $\mathbf{3_{F20Cha}}$ (PDB 7JXN). (A) Cartoon and stick representation of the Phe_{19} face (left) and surface representation of Phe_{19} face (right). (B) Cartoon and stick representation of the Cha_{20} face (left) and surface representation of Cha_{20} face (right). (C) Cartoon representation of the hexamer formed by peptide $\mathbf{3_{F20Cha}}$ (left) and representation showing the hydrophobic core in red (right). Hydrophobic surfaces are highlighted in red.

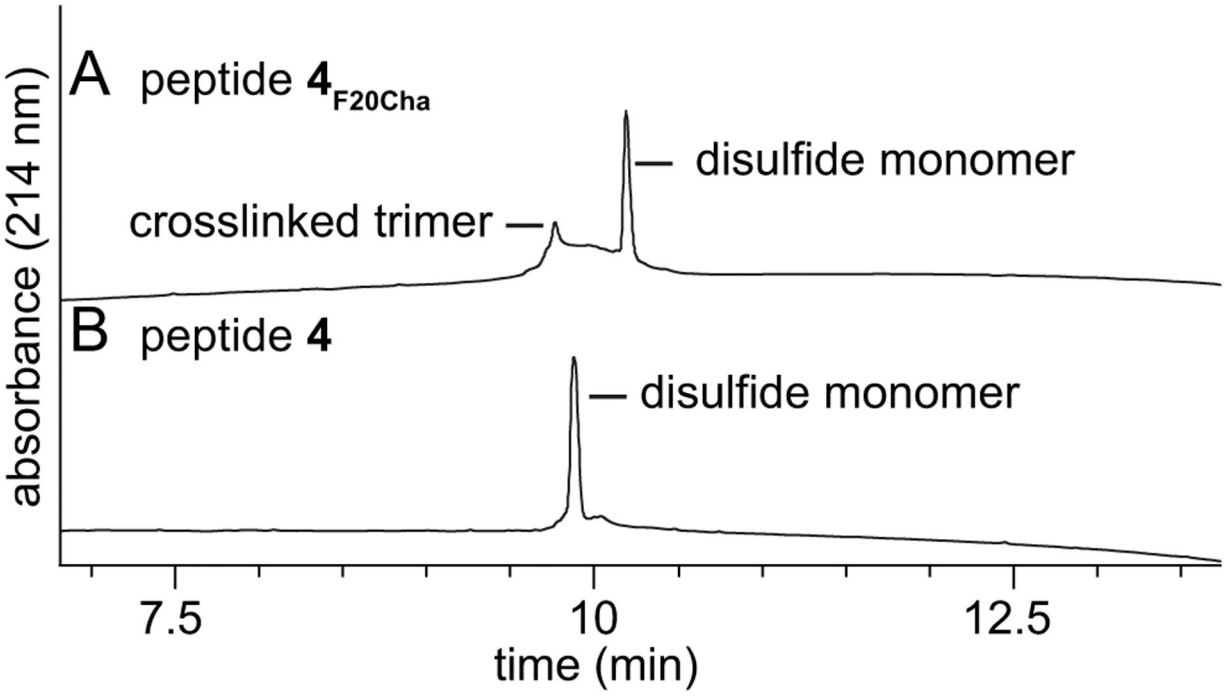

Figure 3.

Oxidation of β-hairpin peptides containing the $A\beta_{24–29}$ loop. (A) HPLC chromatogram of DMSO oxidation of peptide $\mathbf{4_{F20Cha}}$. (B) HPLC chromatogram of DMSO oxidation of peptide **4.** Analytical HPLC was performed on a C18 column with 5–100% elution with acetonitrile over 20 minutes.

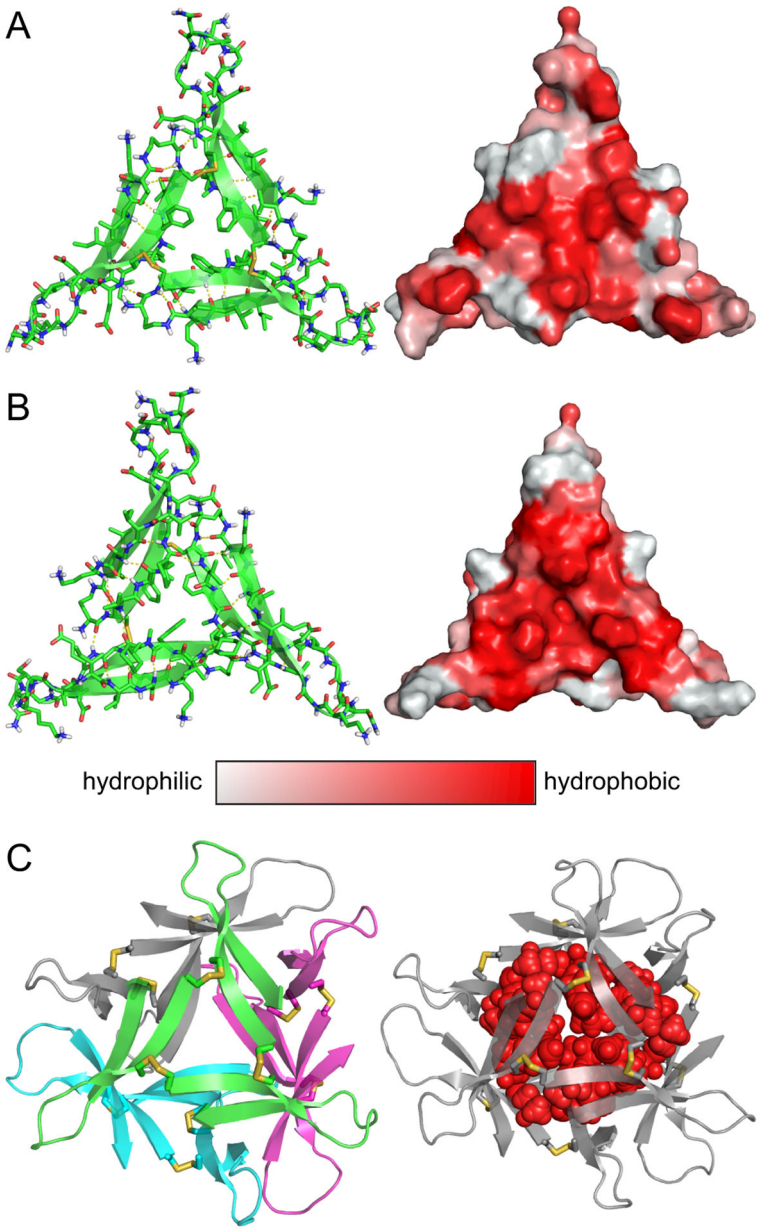

Figure 4.

The X-ray crystallographic structure of trimer $\mathbf{4}_{\mathbf{F20Cha}}$ (PDB 7JXO). (A) Cartoon and stick representation of the Phe_{19} face (left) and surface representation of Phe_{19} face (right). (B) Cartoon and stick representation of the Cha_{20} face (left) and surface representation of Cha_{20} face (right). (C) Cartoon representation of the dodecamer formed by trimer $\mathbf{4}_{\mathbf{F20Cha}}$ (left) and representation showing the hydrophobic core in red (right). Hydrophobic surfaces are highlighted in red.

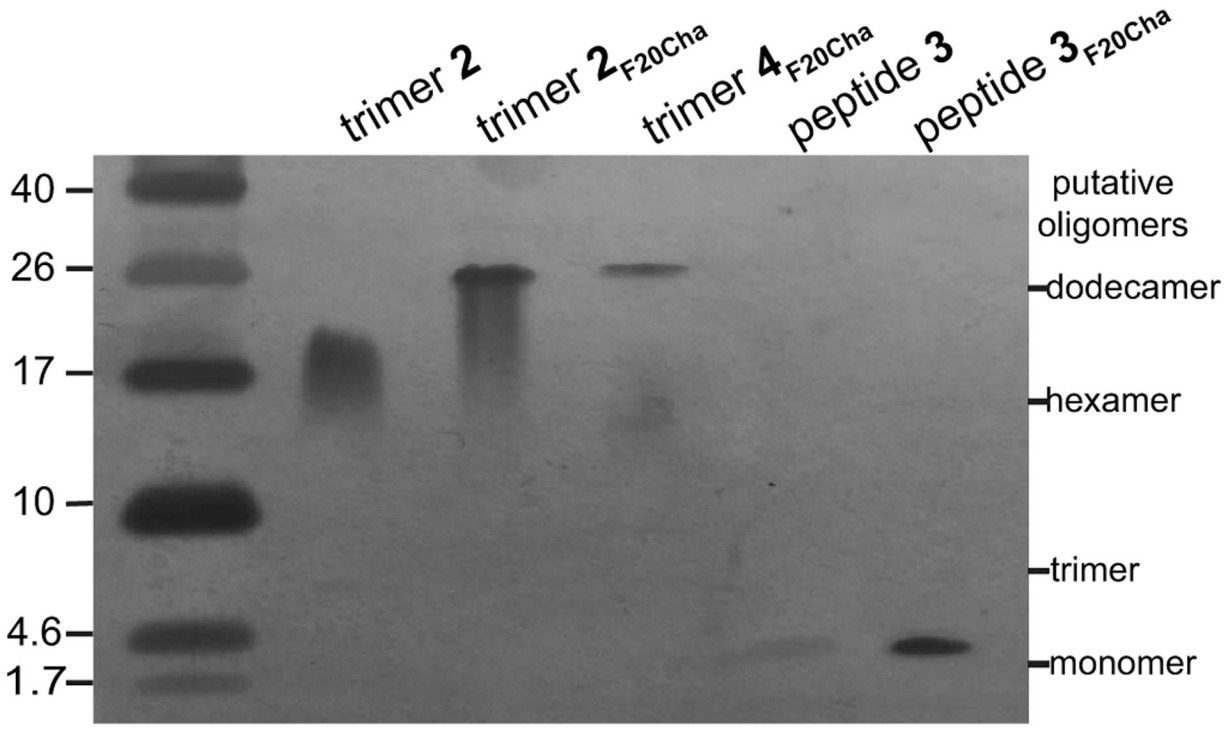

Figure 5.

Silver-stained SDS-PAGE gel. SDS-PAGE was performed on 0.10 mg/mL samples of trimers **2, 2_{F20Cha}**, and **4_{F20Cha}** and 0.30 mg/mL samples of peptides **3** and **3_{F20Cha}** in Tris buffer (pH 6.8) with 2% (w/v) SDS.

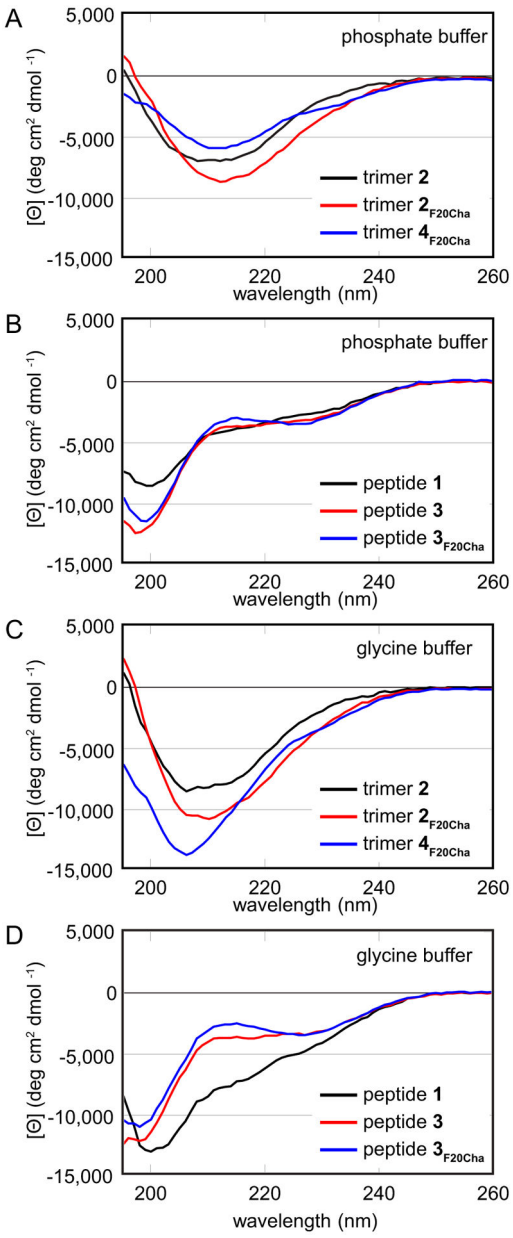

Figure 6.

Circular dichroism spectra. Spectra were acquired at 25 μM for trimers **2**, **2**$_{\mathbf{F20Cha}}$, and **4**$_{\mathbf{F20Cha}}$ and at 75 μM for peptides **1**, **3**, and **3**$_{\mathbf{F20Cha}}$. (A) CD spectra of trimers **2**, **2**$_{\mathbf{F20Cha}}$, and **4**$_{\mathbf{F20Cha}}$ in 10 mM sodium phosphate buffer at pH 7.4. (B) CD spectra of peptides **1**, **3**, and **3**$_{\mathbf{F20Cha}}$ in 10 mM sodium phosphate buffer at pH 7.4. (C) CD spectra of trimers **2**, **2**$_{\mathbf{F20Cha}}$, and **4**$_{\mathbf{F20Cha}}$ in 10 mM glycine buffer at pH 3.0. (D) CD spectra of peptides **1**, **3**, and **3**$_{\mathbf{F20Cha}}$ in 10 mM glycine buffer at pH 3.0.

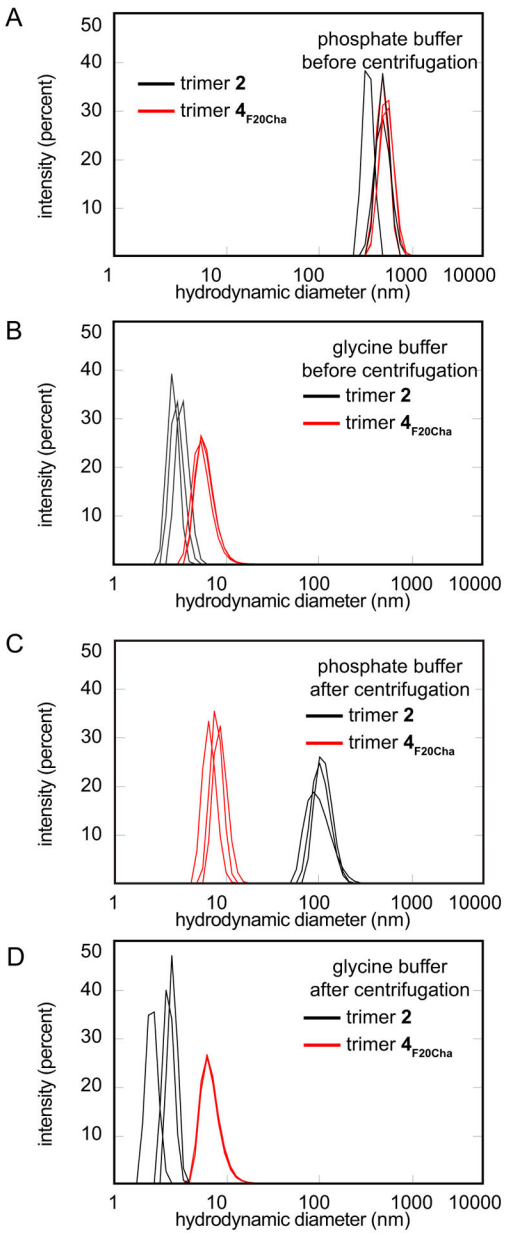

Figure 7.

Dynamic light scattering of trimers **2** and **4$_{F20Cha}$**. (A) DLS of 25 μM solutions of trimmers **2** and **4$_{F20Cha}$** in 10 mM phosphate buffer at pH 7.4 before centrifugation. (B) DLS of 25 μM solutions of trimers **2** and **4$_{F20Cha}$** in 10 mM glycine buffer at pH 3.0 before centrifugation. (C) DLS of 25 solutions of trimers **2** and **4$_{F20Cha}$** in 10 mM phosphate buffer at pH 7.4 after centrifugation. (D) DLS of 25 μM solutions of trimers **2** and **4$_{F20Cha}$** in 10 mM glycine buffer at pH 3.0 after centrifugation.

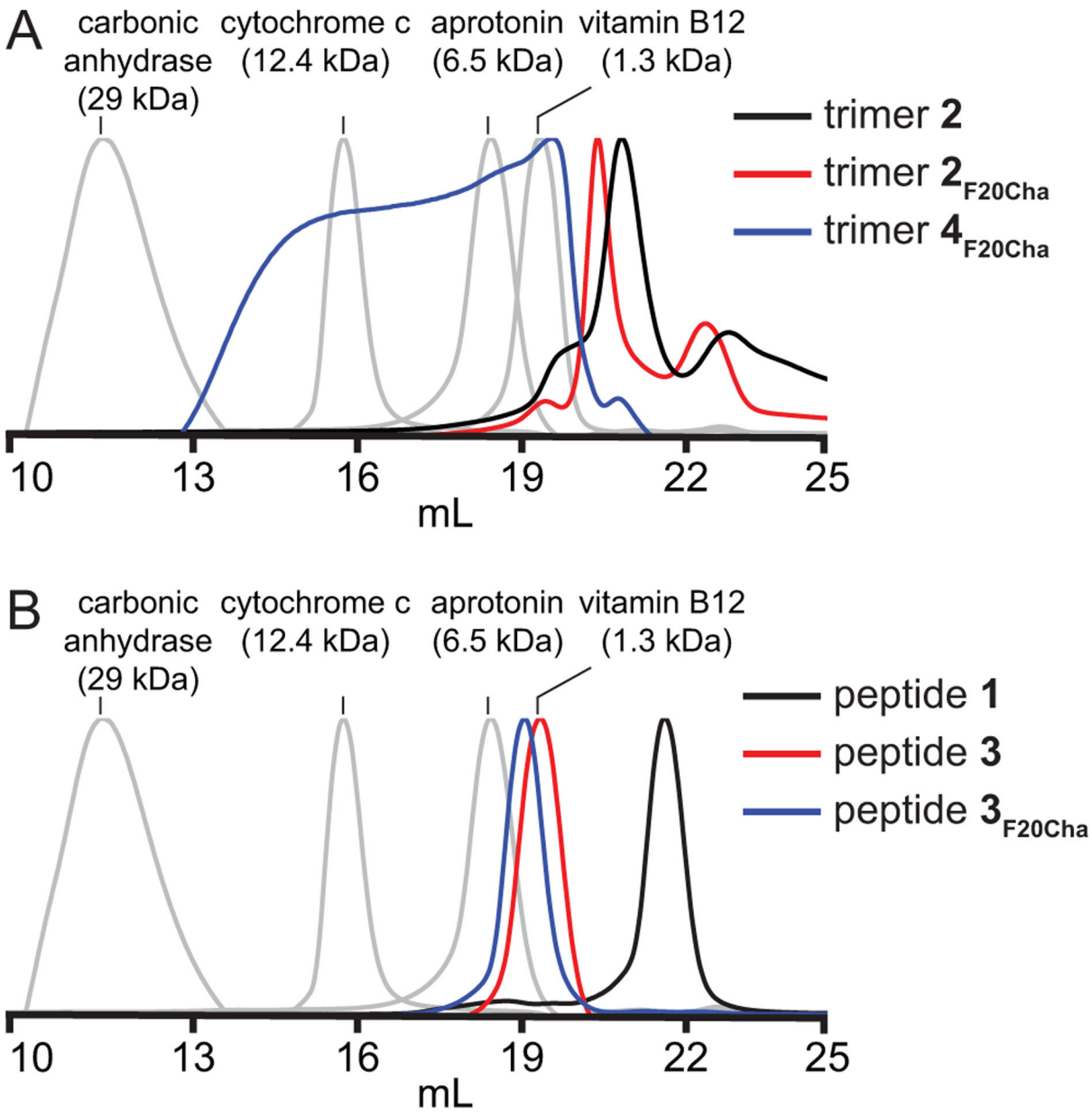

Figure 8.

SEC chromatograms. (A) SEC chromatograms of 1.0 mg/mL solutions of trimers **2**, $\mathbf{2}_{\mathbf{F20Cha}}$, and $\mathbf{4}_{\mathbf{F20Cha}}$. (B) SEC chromatograms of 0.25 mg/mL solutions of peptides **3** and $\mathbf{3}_{\mathbf{F20Cha}}$. Solutions of the trimers and other peptides were dissolved in buffer comprising 10 mM glycine and 50 mM NaCl at pH 3.0ona Superdex 75 10/300 column.

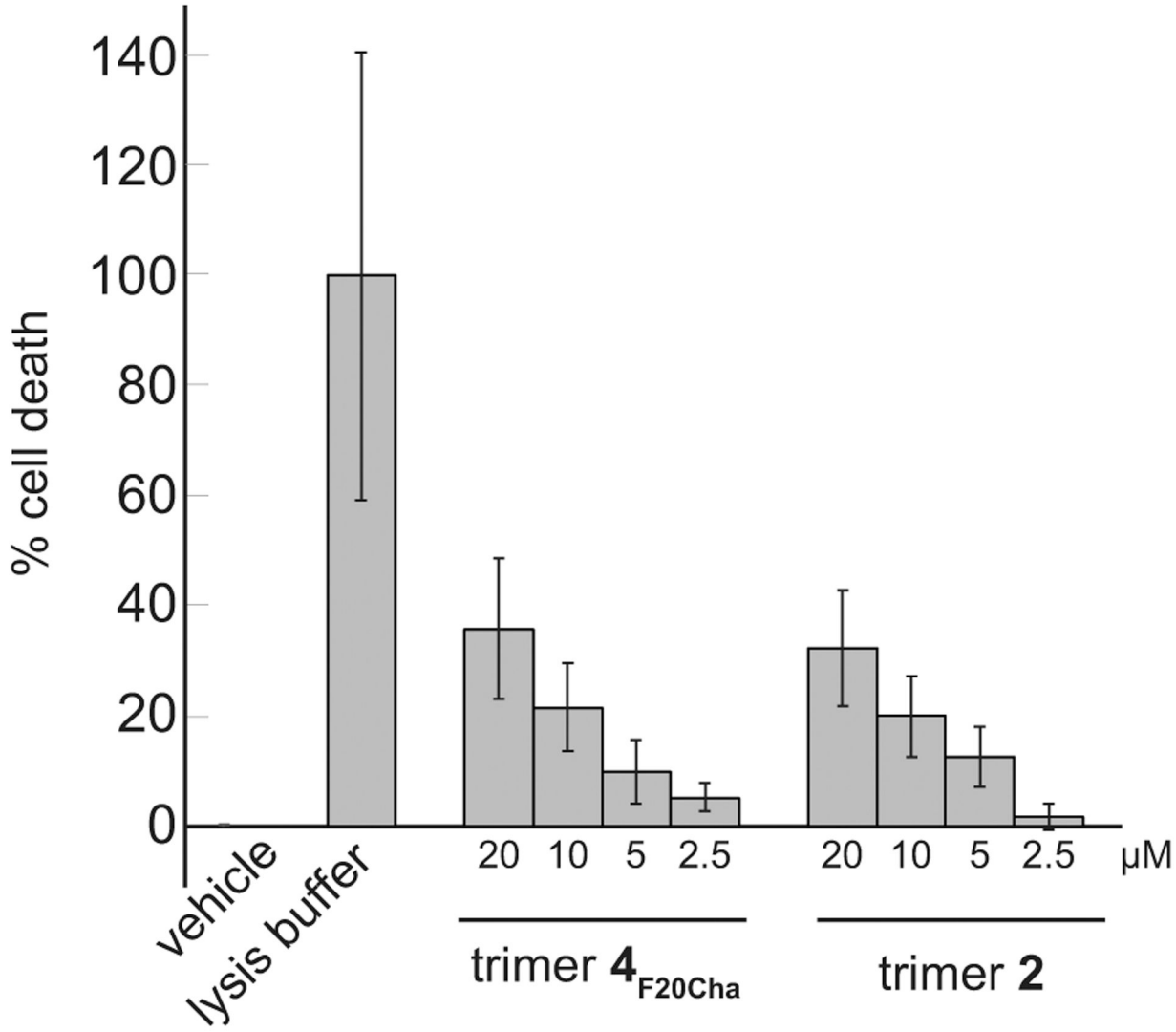

Figure 9.

Cytotoxicity of trimer $\mathbf{4}_{\mathbf{F20Cha}}$ and trimer **2** as assessed by LDH release assay in SH-SY5Y cells. Data represents the mean of six replicate wells, with the error bars corresponding to the standard deviation.

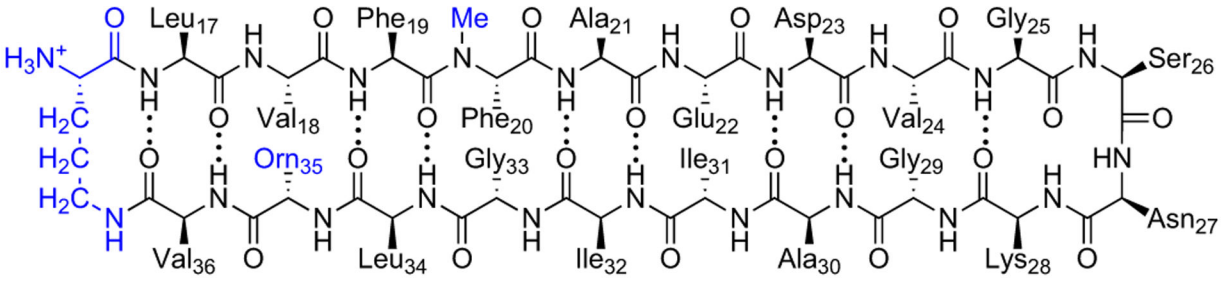

peptide **3**

peptide **3**	cyclo(LVFF$_{Me}$AEDVGSNKGAIIGLOV$^{\delta}$O)
peptide **3**$_{F20Cha}$	cyclo(LVFX$_{Me}$AEDVGSNKGAIIGLOV$^{\delta}$O)
peptide **4**	cyclo(CVFF$_{Me}$CEDVGSNKGAIIGLOV$^{\delta}$O)
peptide **4**$_{F20Cha}$	cyclo(CVFX$_{Me}$CEDVGSNKGAIIGLOV$^{\delta}$O)
trimer **4**	[cyclo(CVFF$_{Me}$CEDVGSNKGAIIGLOV$^{\delta}$O)]$_3$
trimer **4**$_{F20Cha}$	[cyclo(CVFX$_{Me}$CEDVGSNKGAIIGLOV$^{\delta}$O)]$_3$

X = cyclohexylalanine (Cha)

Chart 1.